Supporting Information

Electrografting Amines onto Modified Silver Nanoparticle Electrodes for Electroreduction of CO_2 at Low Overpotential

Maryam Abdinejad,[a] Iranaldo Silva[*b] and Heinz Bernhard Kraatz[*a]

a) Department of Physical and Environmental Sciences, University of Toronto Scarborough, 1265 Military Trail, Toronto, ON M1C 1A4, Canada

b) Departamento de Tecnologia Química, Centro de Ciências Exatas e Tecnologia, Universidade Federal do Maranhão, CEP 65080-805, São Luís, MA, Brasil

Table of Contents:

Part S1. Reagents and Chemicals

All reagents and solvents were of commercial reagent grade and were used without further purification, except where noted. Reagents not listed were purchased from Sigma-Aldrich. *p*-phenylenediamine (99%), sodium nitrite (97%), silver nitrite (99%), and Chloroform d, (> 99.8 %D) were purchased from Sigma-Aldrich. Glassy carbon surface was polished with 1, 0.3 and 0.05 μm alumina slurries, respectively. The electrodes were then ultrasonicated in acetonitrile, ethanol and water. All aqueous solutions were prepared using Millipore water (18.2 M Ω cm).

Part S2. Material Characterizations

^{1}H NMR chemical shifts (δ) were reported in ppm in Deuterium Oxide (D_2O). The NMR data processed in MestReNova software. All the spectroscopy data for structural characterizations were obtained using the research facilities at University of Toronto. The gas product from carbon dioxide (CO_2) electroreduction (CO, H_2) was analysed in 1mL volume using a gas chromatograph (PerkinElmer Clarus 680) coupled with a thermal conductivity detector (TCD) and a flame ionization detector (FID), while the liquid product was analysed using ^{1}H NMR and high-resolution ABI/Sciex Qstar gas chromatography-mass spectrometer (GC-MS).

Surface characterizations were performed using a Hitachi S-5200 Scanning Electron Microscope (SEM, Hitachi, Tokyo, Japan). Transmission Electron Microscopy (TEM) was obtained using a Hitachi H7500 with Olympus SIS MegaView II 1.35MB digital camera and processed with iTEM version 5.2 software. X-ray photoelectric spectroscopy (XPS) analyses were performed with a Theta-probe Thermo-Fisher Scientific Instrument (East Grinstead, UK) with a monochromatic A1 Ka source with a photo energy 1486.6 eV. The accumulated angle was 90° with a 20 eV pass energy at the analyzer at a 8-10 mbar vacuum chamber. The analysis area was 500 μm^2.

Part S3. Electrochemical Measurements

For each electrochemical reaction, the solution was saturated with either CO_2 or Ar and the rest of the experiment was done in a sealed condition. All the electrolysis was done under stirring

conditions. The electrochemical studies were carried out using a CHI 660C potentiostat (CH Instruments, Austin, TX) with a three-electrode set up enclosed in Faraday cage. Glassy carbon and sliver nanotubes (AgNPs) (working electrode), Pt wire (auxiliary) and Ag/AgCl (reference electrode). The electrodes were connected to the cell via a Nafion membrane bridge. Cyclic Voltammetry (CV) measurements were applied with positive initial scan polarity, 5 second quiet and the scan rate of 0.1 V/s. All potentials were reported versus the Ag/AgCl reference electrode. Potentials were changed from Ag/AgCl (3 M KCl) to RHE ($E_{RHE}=E_{Ag/AgCl} + 0.059 \times pH + 0.210$).

The impedance measurements were from 0.1 Hz - 100 kHz frequency range with 10 second quit time, with a sampling rate of 4 points per decade, AC amplitude 10 mV, bias potential 0.28 V. The impedance detection electrolyte was aqueous solution containing 0.2 mol L^{-1} KNO_3 and 2.5×10^{-3} mol L^{-1} $K_3[Fe(CN)_6]/K_4[Fe(CN)_6]$ (1:1) as electroactive probe.

The reported Turn Over Frequencies (TOFs) are average values based on three reaction runs using GC measurements every 15 min for 2 hours. The GC was equipped with a packed Molecular Sieve 5A capillary column and a packed HaySep D column. Helium (99.999%) was used as the carrier gas. A helium ionization detector (HID) was used to quantify H_2 and CO concentrations.

Gas and liquid phases were analyzed by GC. Turnover Numbers (TON) were calculated based on the total amount of the CO products in millimoles (mmol), divided by the total amount of each catalyst in the electrolysis solution (Eq. S1).

Eq. S1:

$$\mathrm{TON} = \frac{n\ (\mathrm{Product})}{n\ (\mathrm{Catalyst})}$$

TOF was calculated using TON divided by the time of the electrolysis (Eq. S2):

Eq. S2:

$$\mathrm{TOF} = \frac{\frac{n\ (\mathrm{Product})}{n\ (\mathrm{Catalyst})}}{\mathrm{t}}$$

Where, n is the total number of millimoles of the product and catalysts in the solution. “t” is the electrolysis time in seconds. n product was calculated based on the number of electrons consumed for reduction of CO_2 to CO and formate (2 electrons), divided by a factor 2F (Eq. S3):

Eq. S3:

$$n\ (\text{product}) = \frac{Q \times \text{FE}}{2F}$$

$n\ Cat$ is calculated based on the following equation (Eq. S4):

Eq. S4:

$$n(Cat) = [Cat] \times Vsol$$

While $[Cat]$ is the concentration of the amine catalysts ($mmol/L$) and $Vsol$ is the volume of the solution (L).

The Faradaic Efficiency (FE) can be calculated via either Eq. S5 or Eq. S6:

Based on Eq. 5, faradaic efficiency of the products was calculated considering the concentration of the achieved products as well as to the two-electron reduction of CO_2 to CO divided by Coulomb as shown below:

Faradaic Efficiency was calculated using Eq. S5:

Eq. S5:

$$\text{FE} = \frac{e_{output}}{e_{intput}} \times 100$$

Where, $e_{\text{output}} = n_{\text{product}} \times$ n (number of electrons) and $e_{\text{input}} =$ Q x t/F (Q= Coulombs)

The Eq. S5 can also be expressed as Eq. S6: FE= Faradic efficiency of the products in percentage (%); Q is the charge in Coulombs (C); n is the number of electrons to produce product), F is Faraday constant (96500 C/mol).

Eq. S6:

$$\text{FE} = \frac{(n_{\text{product}} \times ne \times \text{F})}{(\text{Q} \times \text{t}) \times 100}$$

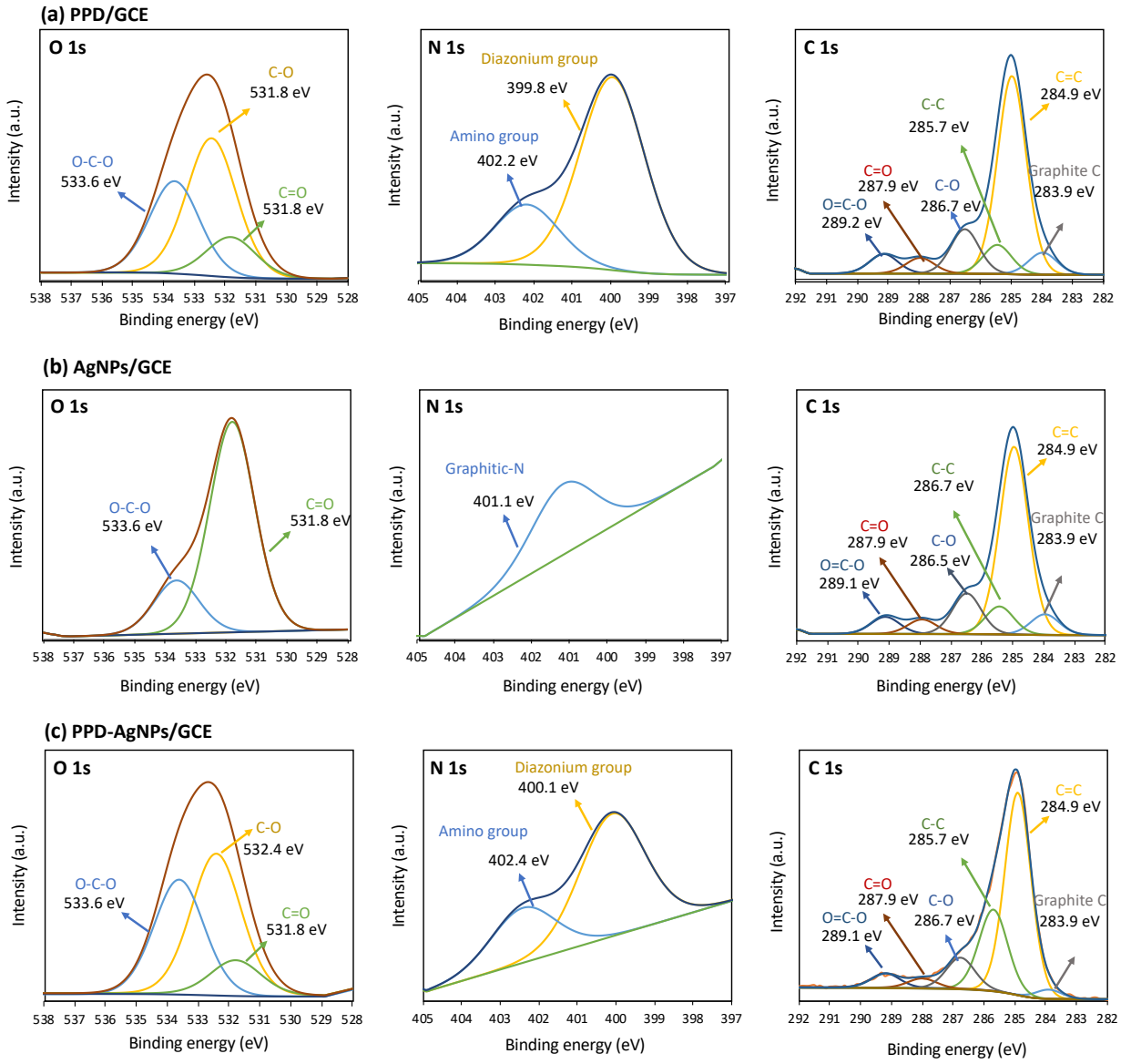

Figure S1: X-ray photoelectron spectroscopy characterization of modified electrode on carbon nanotube. C 1s, N 1s and O 1s spectra of (a) PPD/GCE; (b) AgNPs/GCE; and (c) PPD-AgNPs/GCE.

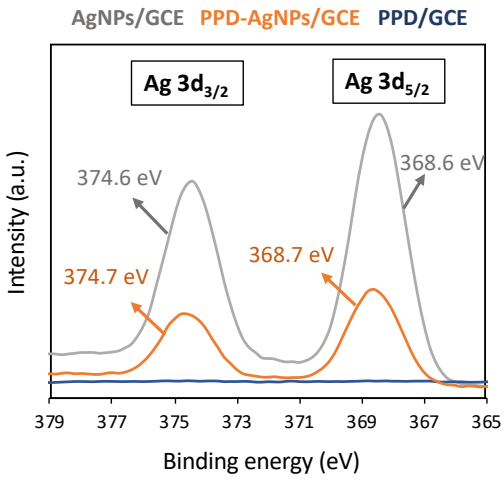

Figure S2: X-ray photoelectron spectroscopy (XPS) Ag 3d spectra comparison of AgNPs/GCE, PPD-AgNPs/GCE and PPD/GCE.

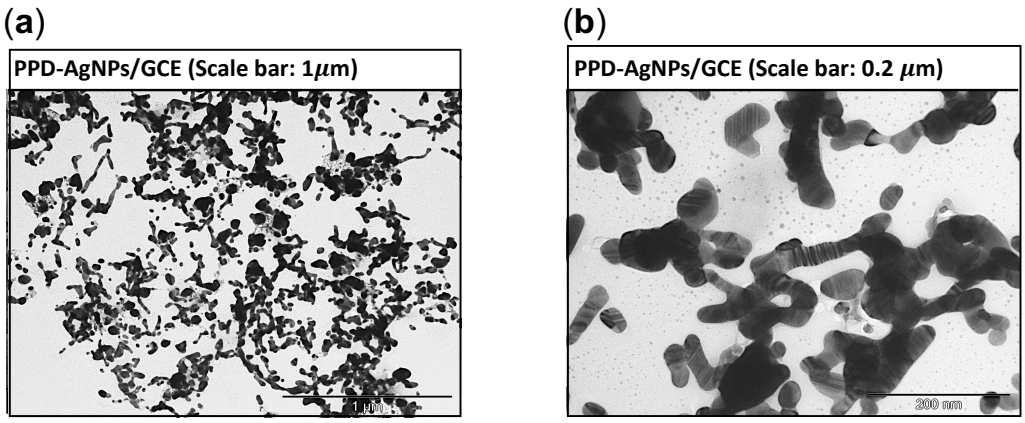

Figure S3. Transmission electron micrograph (TEM) of PPD-AgNPs/GCE with a scale bar of 1 and 0.2 μm, respectively

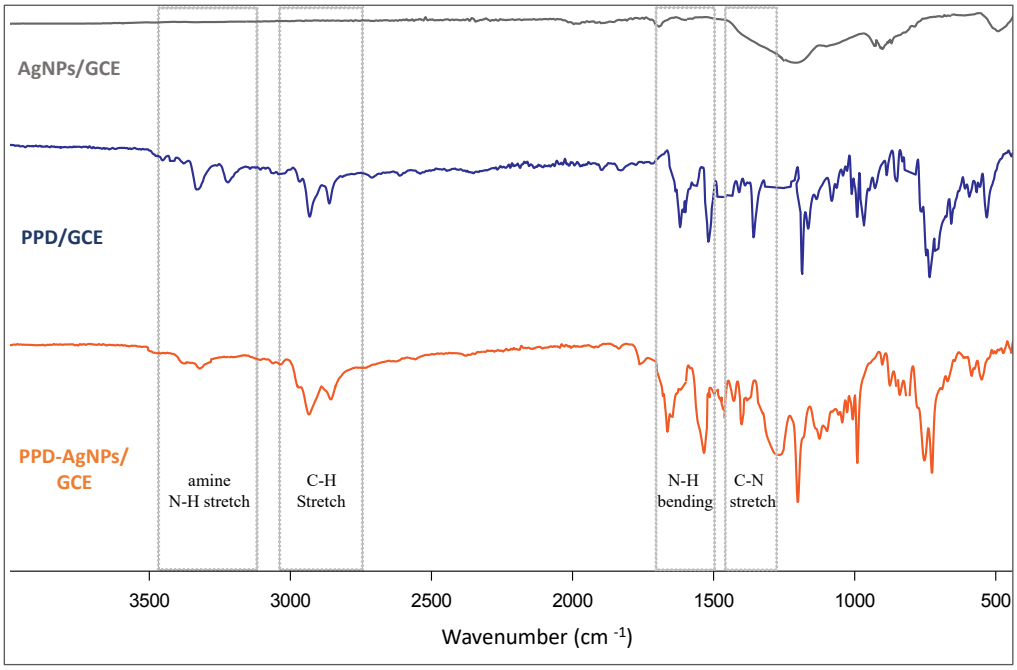

Figure S4. FTIR comparison of AgNPs/GCE, PPD/GCE and PPD-AgNPs/GCE

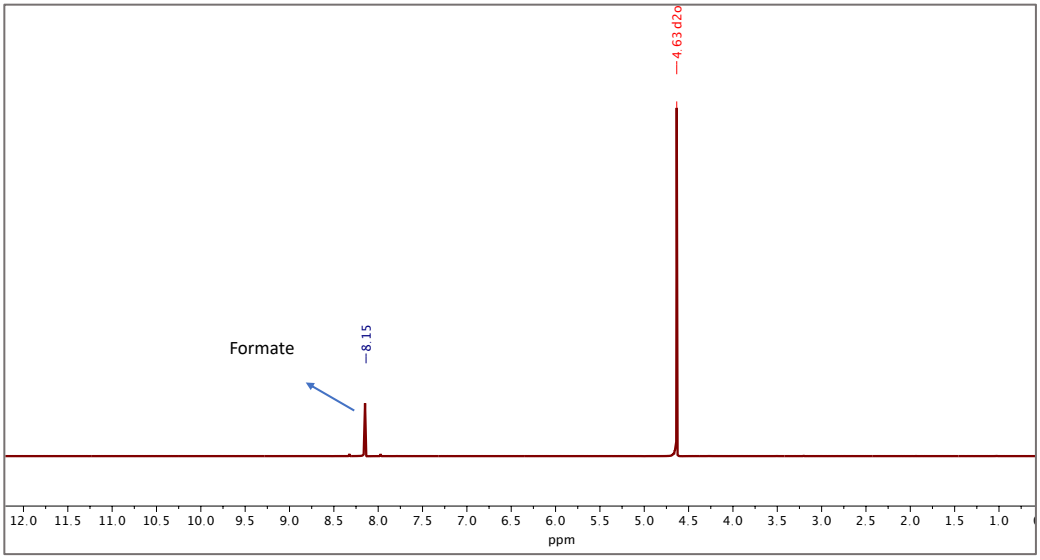

Figure S5. ^{1}H NMR spectra example of PPD/GCE after 2 hours CO_2 electroreduction at 0.2 V vs. RHE in 0.1 M KOH.

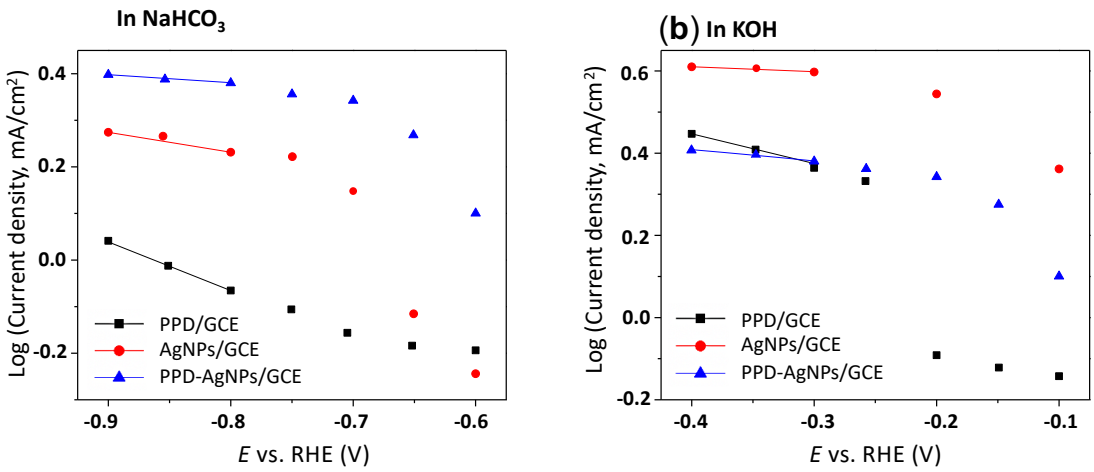

Figure S6. (b) Tafel slopes for the current density of PPD/GCE, AgNPs/GCE, and PPD-AgNPs/GCE in (a) 0.1 M $NaHCO_3$; and (b) in 0.1 M KOH.

Table S1. Product analysis of the different constant potential electrolysis of PPD/GCE, AgNPs/GCE and PPD-AgNPs/GCE for electrochemical CO_2 reduction. The reported data are the average values of six separate measurements from three individual reaction runs at each potential.

Compound	Electrolyte	V vs. RHE	*j* (mA/cm^2)	FE% (CO)	FE% (Formate)	FE% (H_2)	TOF (s^{-1})	Ref.
GCE	$NaHCO_3$ (0.1 M)	-0.8	~ 0.03	-		-	-	Current work
GCE	KOH (0.1 M)	-0.2	-0.23	-	-	100	-	Current work
PPD/GCE	$NaHCO_3$ (0.1 M)	-0.6	-0.64	-	-	100±1.7	0.87	Current work
	$NaHCO_3$ (0.1 M)	-0.7	-0.72	-	14±0.9	84±1	0.09	Current work
	$NaHCO_3$ (0.1 M)	-0.8	-0.86	-	17±1.5	78±1.2	1.0	Current work
	$NaHCO_3$ (0.1 M)	-0.9	-1.1	-	7±1.1	91±1.4	0.92	Current work

Compound	Electrolyte	V vs. RHE	*j* (mA/cm^2)	FE% (CO)	FE% (Formate)	FE% (H_2)	TOF (s^{-1})	Ref.
PPD/GCE	KOH (0.1 M)	-0.1	-0.73	-	6±0.8	93±0.5	1.3	Current work
	KOH (0.1 M)	-0.2	-0.81	-	21±1.3	77±3.4	1.7	Current work
	KOH (0.1 M)	-0.3	-2.2	-	26±1.0	71±2.5	1.4	Current work
	KOH (0.1 M)	-0.4	-2.8	-	20±1.7	79±1.1	1.5	Current work
AgNPs-GCE	$NaHCO_3$ (0.1 M)	-0.6	-0.57	-	-	100±1	-	Current work
	$NaHCO_3$ (0.1 M)	-0.7	- 0.72	11±0.9	-	88±1.6	1.1	Current work
	$NaHCO_3$ (0.1 M)	-0.8	-1.7	38±2.4	-	61±1.3	1.1	Current work
	$NaHCO_3$ (0.1 M)	-0.9	-1.8	27±1.1	-	68±3.2	1.0	Current work
AgNPs-GCE	KOH (0.1 M)	-0.1	-2.3	-	-	100	1.3	Current work
	KOH (0.1 M)	-0.2	-3.5	44±2.1	-	53±3.2	1.2	Current work
	KOH (0.1 M)	-0.3	-3.8	42±1.0	-	57±1.1	1.3	Current work
	KOH (0.1 M)	-0.4	-4.2	35±1.7	-	64±1.9	0.98	Current work
PPD-Ag/GCE	$NaHCO_3$ (0.1 M)	-0.6	-1.2	4±2	9±1.3	85±1.1	2.1	Current work
	$NaHCO_3$ (0.1 M)	-0.7	-2.2	14±1.9	22±1	60±0.7	2.3	Current work
	$NaHCO_3$ (0.1 M)	-0.8	-2.4	17±1.4	37±2	44±1.2	2.8	Current work
	$NaHCO_3$ (0.1 M)	-0.9	-2.5	12±1.5	29±1.2	59±0.9	2.5	Current work

Compound	Electrolyte	V vs. RHE	j (mA/cm^2)	FE% (CO)	FE% (Formate)	FE% (H_2)	TOF (s^{-1})	Ref.
PPD-Ag/GCE	KOH (0.1 M)	-0.1	-5.3	26±1.8	30±2.2	41±1.7	2.9	Current work
	KOH (0.1 M)	-0.2	-6.5	32±2.1	59±1.8	8±1.1	3.3	Current work
	KOH (0.1 M)	-0.3	-6.9	27±1	48±1.9	23±2.7	3.2	Current work
	KOH (0.1 M)	-0.4	-7.6	20±1.2	32±1.3	47±3.1	3.1	Current work
Ag electrode	$CsHCO_3$ (0.1 M)	-1.0	-5.8	80	-	-	-	[1]
AgNPs	EMIN-BF_4	N/A	-0.61	96	-	4	-	[2]
AgNPs	$KHCO_3$ (0.1 M)	-0.7	-0.4	45	-	18	-	[3]
Ag foil	$KHCO_3$ (0.1 M)	-0.8	-0.01	2.2	-	75	-	[3]
Ag Nano-coarals	$KHCO_3$ (0.1 M)	-0.7	-6.6	95	-	4	-	[3]
Nanoporous Ag	$KHCO_3$ (0.5 M)	-0.8	-0.19	92	-	7	-	[4]
Ag Compact grains	$KHCO_3$ (0.1 M)	-1.1	-5.7	88.9	-	-	-	[5]
Ag Plate	$KHCO_3$ (0.1 M)	-1.12	-22.9	79.0	-	-	-	[6]
Ag foam	$KHCO_3$ (0.1 M)	-1.12	-27.43	82.9	-	-	-	[6]
Ag Truncated hexagonal bipyramidal	$KHCO_3$ (0.1 M)	-0.93	-4.92	89.4	-	-	-	[7]
L25-Ag nanocubes	$KHCO_3$ (0.1 M)	-0.85	-1.7	99	-	-	-	[8]
D-25 Ag NWs (diameter less than 25 nm)	$KHCO_3$ (0.1 M)	-0.96	-3.2	99	-	-	-	[9]

Compound	Electrolyte	V vs. RHE	*j* (mA/cm^2)	FE% (CO)	FE% (Formate)	FE% (H_2)	TOF (s^{-1})	Ref.
Ag NWs (35 nm)	$KHCO_3$ (0.5 M)	-0.9	-7	80	-	-	-	[10]
Ag NWs (200 nm)	$KHCO_3$ (0.5 M)	-0.7	-12.2	84	-	-	-	[11]
6 μm thick highly porous Ag	$KHCO_3$ (0.5 M)	-0.5	-10.5	82	-	-	-	[12]
Sponge-like porous Ag	$KHCO_3$ (0.1 M)	-0.9	-7	93	-	-	-	[13]
Ag nanosheets	$KHCO_3$ (0.5 M)	-0.6	-1.6	90	-	-	-	[14]
AgCl-derived Ag	NaCl (3.5%)	-1.1	-7.5	90	-	-	-	[15]
Ag_3PO_4-derived Ag	$KHCO_3$ (0.5 M)	-0.7	-2.93	97.3	-	-	-	[16]
Iodide-derived Ag	$KHCO_3$ (0.5 M)	-0.7	-16.7	94.5	-	-	-	[17]
Ag2P nano crystals	$KHCO_3$ (0.5 M)	-0.8	-7.5	82	-	-	-	[18]
cysteamine AgNPs	$KHCO_3$ (0.5 M)	-0.75	-3.8	84.4	-	-	-	[19]
Benzenethiolate -modified	$KHCO_3$ (0.1 M)	-1.03	-502/g	96	-			[20]
Polycrystalline Ag	$KHCO_3$ (0.5 M)	-0.75	-1.0	70.5	-	28	-	[19]
polycrystalline Ag electrode	$NaNO_3$ (0.1 M)	-0.6	-3.7	92.8	-	-	-	[21]
Thiol Modified Ag/C	$KHCO_3$ (0.5 M)	-1.0	-0.15	65.5	-	35	-	[22]
Amine Derived-Pb	$KHCO_3$ (1 M)	-1.09	-9.5	94	-	6	-	[23]

Table S2. Equivalent circuit parameters resulting from the fitting of impedance data

Surface	Rs (Ohm)	Rct (Ohm)	CPE (μF)
GCE	63.42 ± 1.39	147.6 ± 3.46	1.76 ± 0.21
AgNPs	84.39 ± 1.29	544.7 ± 23.9	4.95 ± 0.68
PPD/GCE	59.27 ± 1.60	1285 ± 73.6	2.93 ± 0.39
AgNPs-PPD/GCE	63.23 ± 1.60	693.6 ± 38.5	4.57 ± 0.76

References:

1 M. R. Singh, Y. Kwon, Y. Lum, J. W. Ager and A. T. Bell, *J. Am. Chem. Soc.*, 2016, **138**, 13006–13012.

2 B. a Rosen, A. Salehi-khojin, M. R. Thorson, W. Zhu, D. T. Whipple, P. J. a Kenis and R. I. Masel, *Science*, 2011, **334**, 643–644.

3 Y.-C. Hsieh, S. D. Senanayake, Y. Zhang, W. Xu and D. E. Polyansky, *ACS Catal.*, 2015, **5**, 5349–5356.

4 Q. Lu, J. Rosen, Y. Zhou, G. S. Hutchings, Y. C. Kimmel, J. G. Chen and F. Jiao, *Nat. Commun.*, 2014, **5**, 3242.

5 Q. Jianping, T. Juntao, S. Jie, W. Cuiwei, Q. Mengqian, H. Zhiqiao, C. Jianmeng and S. Song, *Electrochim. Acta*, 2016, **203**, 99–108.

6 Y. Yu, N. Zhong, J. Fang, S. Tang, X. Ye, Z. He and S. Song, *Catalysts*, 2019, 9, 57.

7 Z. He, T. Liu, J. Tang, C. Zhou, L. Wen, J. Chen and S. Song, *Electrochim. Acta*, 2016, **222**, 1234–1242.

8 S. Liu, C. Sun, J. Xiao and J.-L. Luo, *ACS Catal.*, 2020, **10**, 3158–3163.

9 S. Liu, X.-Z. Wang, H. Tao, T. Li, Q. Liu, Z. Xu, X.-Z. Fu and J.-L. Luo, *Nano Energy*, 2018, **45**, 456–462.

10 W. Xi, R. Ma, H. Wang, Z. Gao, W. Zhang and Y. Zhao, *ACS Sustain. Chem. Eng.*, 2018, **6**, 7687–

7694.

11 C. Luan, Y. Shao, Q. Lu, S. Gao, K. Huang, H. Wu and K. Yao, *ACS Appl. Mater. Interfaces*, 2018, **10**, 17950–17956.

12 L. Zhang, Z. Wang, N. Mehio, X. Jin and S. Dai, *ChemSusChem*, 2016, **9**, 428–432.

13 T. Fan, Q. Wu, Z. Yang, Y. Song, J. Zhang, P. Huang, Z. Chen, Y. Dong, W. Fang and X. Yi, *ChemSusChem*, 2020, **13**, 2677–2683.

14 C.-Y. Lee, Y. Zhao, C. Wang, D. R. G. Mitchell and G. G. Wallace, *Sustain. Energy Fuels*, 2017, **1**, 1023–1027.

15 C.-Y. Lee and G. G. Wallace, *J. Mater. Chem. A*, 2018, **6**, 23301–23307.

16 J. Gao, C. Zhu, M. Zhu, Y. Fu, H. Huang, Y. Liu and Z. Kang, *ACS Sustain. Chem. Eng.*, 2019, **7**, 3536–3543.

17 Y. Zhang, L. Ji, W. Qiu, X. Shi, A. M. Asiri and X. Sun, *Chem. Commun.*, 2018, **54**, 2666–2669.

18 H. Li, P. Wen, D. S. Itanze, Z. D. Hood, X. Ma, M. Kim, S. Adhikari, C. Lu, C. Dun, M. Chi, Y. Qiu and S. M. Geyer, *Nat. Commun.*, 2019, **10**, 5724.

19 C. Kim, H. S. Jeon, T. Eom, M. S. Jee, H. Kim, C. M. Friend, B. K. Min and Y. J. Hwang, *J. Am. Chem. Soc.*, 2015, **137**, 13844–13850.

20 S. C. Abeyweera, J. Yu, J. P. Perdew, Q. Yan and Y. Sun, *Nano Lett.*, 2020, **20**, 2806–2811.

21 L. Q. Zhou, C. Ling, M. Jones and H. Jia, *Chem. Commun.*, 2015, **51**, 17704–17707.

22 C. Kim, T. Eom, M. S. Jee, H. Jung, H. Kim, B. K. Min and Y. J. Hwang, *ACS Catal.*, 2017, **7**, 779–785.

23 N. Zouaoui, B. D. Ossonon, M. Fan, D. Mayilukila, S. Garbarino, G. de Silveira, G. A. Botton, D. Guay and A. C. Tavares, *J. Mater. Chem. A*, 2019, **7**, 11272–11281.